Acrylonitrile-Based Copolymers: Synthesis, Characterization, and Formation of Ultrafiltration Membranes Utilized for the Immobilization of Proteins

PAUL I. DALVEN,* JAMES R. HILDEBRANDT,† ABRAHAM SHAMIR,‡ ANTHONY J. LACCETTI,§ LEONARD T. HODGINS,¶ and HARRY P. GREGOR,** *Department of Chemical Engineering and Applied Chemistry, Columbia University, New York, New York 10027*

Synopsis

Various high molecular weight copolymers of acrylonitrile and a vinyl comonomer containing an aryl amine, a pyridine, or an aliphatic hydroxyl group were synthesized via slurry polymerization techniques so as to contain from 1 to 15 mol % functional comonomer. The comonomer content was quantitated by ultraviolet absorbance, base titration of acid polymer salts, and/or relative chemical reactivity with trichloro-*s*-triazine. Thin films were cast from copolymer solutions, coagulated into unsupported ultrafiltration membranes, and characterized with respect to both water permeability and pore size distribution. Analysis by size exclusion chromatography of the membrane permeate of a pool of dextran fractions yielded a continuous distribution curve for membrane pore size over the range 1.5 to 70 nm. The ultrafiltration membranes were used for protein immobilization after appropriate chemical activation. The three distinct types of functional copolymers gave comparable results for α-chymotrypsin, with protein weight loadings of 6–12% and 40–65% retention of enzymatic specific activity.

INTRODUCTION

Numerous enzymes have been attached to insoluble supports by a variety of chemical coupling techniques, and the subject has been extensively reviewed.[1,2] Typically, enzymes are immobilized upon solid particles or porous beads for use as catalysts in a packed bed reactor configuration. The immobilization of enzymes upon the pore surface of a membrane, however, offers a number of advantages over packed bed systems, especially when operated in the form of a pressure-driven spiral-wound module. Such membrane modules are judged superior to packed beds with respect to enzyme loading, operational stability of the enzyme reactor, external and internal diffusional efficiency, throughput per unit area, and residence time distribution.[3]

* Present Address: Israel Desalination Eng. Ltd., P.O.B. 18041, Tel Aviv 61180, Israel.

† Present Address: 560 Riverside Drive, #20 N, New York, NY 10027.

‡ Present Address: Schering-Plough Corp., Bioisolation Dept., 1011 Morris Ave., Union, NJ 07083.

§ Present Address: Dorr-Oliver Inc., 77 Havemeyer Lane, Stamford, CN 06904.

¶ Present Address: New York University, Dept. of Biochemistry, College of Dentistry, New York, NY 10010.

** Author to whom to address all correspondence.

Journal of Applied Polymer Science, Vol. 30, 1113–1132 (1985)
 CCC 0021-8995/85/031113-20$04.00

Membranes composed of natural polymers such as cellulose or protein have been used for the immobilization of enzymes,[4-6] but are susceptible to degradation by microbes and enzymes.[7] Relatively few noncellulosic or nonproteinaneous membranes have been employed as carriers for protein immobilization. Examples include membranes made from a blend of polysulfone and aminopolysulfone,[8,9] from nylon-coated polyethylene sheets,[10] and from polyethyleneimine-coated poly(vinyl chloride)–silica sheets.[11]

Polymers of acrylonitrile have been used but infrequently for enzyme immobilization. For example, proteins have been ionicly bound to an acrylonitrile homopolymer after partial derivatization of the nitriles to imidoesters[12-14]; the derivatized polymer, however, bound only a small amount of protein. The photografting of *N,N*-dimethylaminoethyl methacrylate onto PAN that had been polymerized in the presence of bromoform also led to a support used for the ionic immobilization of the enzyme urease only after the quaternization of the amines.[15] In addition, the introduction of amines into PAN by partial reduction of nitrile groups facilitates adsorption of proteins onto the support and subsequent crosslinking with glutaraldehyde into a stable network.[16] Such supports are inferior since they require activation/coupling chemistries that are not versatile and/or that result in weak covalent bonds, which cannot prevent subsequent leakage of enzyme due to solvolytic processes.[17,18]

In order to circumvent such problems, we have developed a series of ultrafiltration membranes based on synthetic copolymers "tailor-made" for specific types of enzyme coupling reactions. Acrylonitrile (AN) was chosen as the predominant comonomer due to the relative ease of copolymerization of AN with a wide variety of comonomers and the excellent film forming character of polyacrylonitrile (PAN). A monomer containing either an aryl amine, hydroxyl, or pyridine group was copolymerized with AN to allow the employment of a variety of activation/coupling chemistries for enzyme immobilization. The synthesis of these copolymers and the characterization of membranes made from them are the subjects of this report.

MATERIALS AND METHODS

Materials

The following chemicals were purchased from Aldrich Chemical Co.: 3-(α-hydroxyethyl)aniline (HEA), 4-(2-aminoethyl)pyridine, 4-ethylpyridine, *m*-ethylaniline, *p*-ethylaniline, acryloyl chloride, methacryloyl chloride, 2,6-di-*tert*-butyl-4-methylphenol (BHT), trichloro-*s*-triazine (TsT), *N,N*-diisopropylethylamine (DIPEA), and 1,3-di-*O*-tolylguanidine (DTG). Acrylonitrile, 2,2′-azobis(2-methylpropionitrile) (AIBN) and *p*-methoxyphenol (MEHQ) were obtained from Eastman Kodak Co. Other chemicals and their vendors included: alumina F1, 14-28 mesh (Alcoa Chemical); *N,N*-di-2-naphthyl-*p*-phenylene diamine (Pfaltz & Bauer); *N*-(9-hydroxy-4,7-dioxa-nonyl)amine (polyglycolamine H-163, from Union Carbide); triethylamine, acetic anhydride, ethylenediamine (EDA), ethylene carbonate (EC), propylene carbonate (PC), *N,N*-dimethylformamide (DMF), and cyanogen bromide (Fisher

Scientific); acrylic acid (Dow Badische Chemical Co.); polyacrylonitrile, (PAN, type A homopolymer, from DuPont); 2-(2-aminoethoxy)ethanol (diglycolamine, from Texaco Chemical Co.); 4-vinylpyridine (4VP, from Reilly Tar & Chemical Co.); *p*-aminostyrene (pAS, from Fairfield Chemical Co.); and Amberlite IRA-900 and IRC-50 (Rohm & Haas). Bovine α-chymotrypsin (CT), blue dextran, ε-amino-*n*-caproic acid (EACA), glutaryl-L-phenylalanine-*p*-nitroanilide (GPNA), and dextran fractions of average molecular weight 10,500, 17,700, 40,000, 70,300, 252,000, and 2,000,000 were supplied by Sigma Chemical Co. A dextran fraction of molecular weight 4000–6000 was obtained from Accurate Chemical. Polystyrene calibration standards were the products of Waters Associates or Polysciences Inc. Acrylonitrile was freshly distilled before use after being made acidic with phosphoric acid.

Methods

Synthesis of *m*-Aminostyrene (mAS)

mAS was prepared by a protocol modified from that of Petit and Lumbroso[19] for pAS. HEA (50 g) was melted at 80°C and added dropwise to 50 mL of solid alumina granules heated to about 300°C, 10–15 torr, in a three-neck round-bottom flask equipped with a heated addition funnel, a thermometer, and a water condenser/receiving flask; the receiving flask contained 2–5 mg of the nonvolatile polymerization inhibitor, *N,N*-di-2-naphthyl-*p*-phenylene diamine. Care was taken to avoid an excessive rise in temperature during the addition of HEA onto the alumina. Prior to use, the product was removed from the starting material, inhibitor, and water by vacuum distillation at 20 torr through a Vigreaux column. The colorless product in a 50% yield was collected at 52–56°C and stored at −20°C. Reverse phase ion-pair chromatography on a Sperisorb-C6 column showed that over 98% of the material absorbing at 280 nm eluted in one peak, with only a minor nonabsorbing peak as detected by refractometry.

Synthesis of *N*-(5-Hydroxy-3-oxa-pentyl)methacrylamide (HOPMAM), *N*-(5-Hydroxy-3-oxa-pentyl)acrylamide (HOPAM), and *N*-(9-Hydroxy-4,7-dioxa-nonyl)methacrylamide (HDNMAM)

Three hydroxy-containing vinyl monomers were synthesized by minor variations on the following scheme. A mixture of 500 mL absolute ethanol, 1.0 mol (101 g) triethylamine, 0.2 g MEHQ, and 1.0 mol (105 g) diglycolamine (or 1.0 mol, 163 g, polyglycolamine) was dried thoroughly over 3-Å molecular sieves and filtered through a 0.45-μm cellulose acetate membrane filter into a three-neck round-bottom flask equipped with an addition funnel, thermometer, and a nitrogen inlet. The flask was cooled to −50°C by immersion in a dry ice/alcohol bath while under a nitrogen atmosphere; 1.0 mol (105 g) of methacryloyl chloride or 1.0 mol (90.5 g) acryloyl chloride was then added slowly, accompanied by overhead mechanical stirring. After the temperature was allowed to increase to −20°C, a triethylamine–HCl precipitate was removed by filtration through paper on a jacketed Buchner funnel maintained at −10°C. The filtrate was pooled with a 100 mL −20°C ethanol

wash of the precipitate and passed through a Amberlite IRA-900 column to remove chloride ions. The effluent was checked for the absence of chloride ions with 1% $AgNO_3$ in 1*N* HNO_3. After rinsing the column with ethanol, 0.2 g of MEHQ was added to the column effluent/wash pool, which was subsequently concentrated on a rotary evaporator to about 160 g; this concentration step also removed residual triethylamine. The concentrate was diluted with 250 mL of ethanol and repurified by passage through an Amberlite IRC-50 column to remove residual amines. The effluent was pooled with a 250 mL ethanol rinse of the column, and after the addition of 0.2 g MEHQ, it was concentrated and dried under high vacuum. The yield was between 80% and 85% for all three acrylamides.

Synthesis of *N*-(2-(4-Pyridyl)ethyl)acrylamide (PEAM)

This substituted acrylamide was synthesized from acrylic anhydride and 4-(2-aminoethyl)pyridine. Acrylic anhydride was obtained from acrylic acid and acetic anhydride as described.[20] Synthesis of PEAM was initiated by the slow addition of 0.36 mol (45.0 g) of acrylic anhydride in 50 mL of ethyl ether containing 50 mg of BHT to 0.35 mol (42.76 g) of 4-(2-aminoethyl)pyridine in 150 mL of ethyl ether containing 150 mg of BHT at −55°C, with the formation of a precipitate. The rate of addition was kept sufficiently slow to ensure that the temperature did not exceed −30°C during the reaction. After removal of the ether by room temperature evaporation, the precipitate was dissolved in 200 mL of methanol and subsequently vacuum distilled. The substituted acrylamide (15% yield) was collected at 170°C, 100 mtorr.

Copolymerization of Acrylonitrile with *N*-Substituted Acrylamides, *N*-Substituted Methacrylamides, or 4-Vinylpyridine

These copolymerizations were performed as an aqueous slurry[21] at pH 3.2 with a total monomer concentration of 1.4*M*. The reactions were done under nitrogen in a resin kettle equipped with a turbine stirrer and an internal cooling coil. A reaction was initiated by the addition of ammonium peroxydisulfate (0.02% final concentration) and sodium metabisulfate (0.1% final concentration); the temperature was thermostatted at 50 ± 0.3°C. An 80% conversion was typically achieved by 2–3 h. The polymer was isolated by vacuum filtration, washed with water (or 1.0*M* NH_4OH for a pyridine containing copolymer), dispersed in a blender, collected again by filtration, and dried at 50°C under vacuum.

Copolymerization of Acrylonitrile with *m*- or *p*-Aminostyrene

Copolymerization was performed in 50% methanol using AIBN as the initiator. For example, 3.0 g pAS was dispersed in 120 mL of water and concentrated HCl was added until the amine became fully dissolved. The solution was then treated with activated charcoal to remove colored contaminants. After filtration to remove the charcoal, the pH was adjusted to 1.1 with concentrated HCl, and 125 mL of methanol was added. The solution was transfered to a three-neck round-bottom flask equipped with a subsurface nitrogen inlet, a thermometer, a mechanical stirrer, and a reflux condenser. Distilled acrylonitrile (65 mL, 53 g) and 150 mg AIBN was added

with stirring; the system was purged with nitrogen throughout. The temperature was then brought to and maintained at 50°C. The reaction proceeded rapidly, and, after 20 h, 50 mL of 50% methanol was added to thin the slurry. After a total of 48 h, 50 mL of 1.0*M* NH_4OH was added, and the polymer collected by filtration. Following blending in 1.0*M* NH_4OH and washing with ethanol, the polymer was dried under vacuum at 40°C. A 70% conversion was typical.

Viscosity Measurements

Viscosity measurements were made in a thermostatted water bath at 30 ± 0.1°C using a Ubbelohde viscometer. A copolymer was dissolved in DMF which had been exhaustively dried over molecular sieves. For each polymer, the viscosity of a minimum of three concentrations was measured such that t/t_0, the ratio of flow time for copolymer solution to solvent, was between 1.1 and 1.6; multiple readings were made at each concentration. Intrinsic viscosity was obtained by extrapolation of a plot of specific viscosity/concentration vs. concentration to infinite dilution using linear least squares; such analysis yielded regression coefficients ≥ 0.999. Estimates of the copolymer molecular weight were obtained from the relationship for PAN in DMF at 25°C[22]:

$$[\eta] = 2.33 \times 10^{-4} M_w^{0.75}$$

where $[\eta]$ is the intrinsic viscosity and M_w is the weight-average molecular weight.

Acid-Base Titration of Polymeric Aryl Amines and Pyridines

A DMF solution of a copolymer was cast as a thin film, coagulated in methanol, and dried *in vacuo*. To about 2.0 g of copolymer redissolved in 30 mL of DMF, 0.6 mL of concentrated NH_4OH was added. After overnight stirring, the copolymer was precipitated with (1:1) methanol:0.1*N* NH_4OH, filtered, washed with ethanol, and dried *in vacuo*. This rigorous washing/coagulation scheme was required to remove all traces of titratable reactants and water-soluble low-molecular-weight polymer chains; the polymer is left in its free base form after this protocol. About half of this dried material was dissolved in 30 mL DMF, and the perchlorate salt was formed by the addition of 0.3 mL of 70% perchloric acid. The polymer salt then was coagulated in ethanol, washed with ethanol, and dried *in vacuo*. A known weight of the dried polymer salt was dissolved in 70 mL distilled DMF and titrated with 0.05*M* DTG in DMF[23] using a Fisher Accumet pH meter equipped with a glass body combination electrode. The exact concentration of the DTG solution was determined by titration with standardized 0.1*N* HCl; before use, DMF was distilled from NaOH as described.[24]

The number of titratable groups in a coagulated membrane was measured by back-titration of the amount of acid displaced from a membrane previously converted into its acid salt. A 47 mm diameter membrane disk was soaked extensively in 1.0*N* HCl and washed well with ethanol to remove unbound acid. The HCl was then displaced by soaking the membrane in 10 mL of 0.01*N* Na_2CO_3 for 1 h. After washing the membrane nine times with

10 mL portions of water, all washes were pooled with the soaking solution and titrated with 0.01*N* HCl. As a control, an equal volume of carbonate solution unexposed to a membrane was also titrated. The difference between the two titration values was assigned to solvent-accessible, acid-titratable groups in the membrane.

Spectrophotometric Analysis of Polymeric Aryl Amines and Pyridines

Absorbance spectra of 0.5 mg/mL solutions of copolymers in spectra grade DMF or EC-PC (3:1, v/v) were recorded on a Gilford 2600 microprocessor controlled spectrophotometer. Prior to scanning, aryl amine copolymer solutions were made basic with NH_4OH. The molar extinction coefficient (ϵ_M) at the wavelength of maximum absorbance (λ_{max}) of the model compounds used to estimate the polymeric incorporation of pAS, mAS, and 4VP are, respectively: *p*-ethylaniline in DMF, 0.43*M* NH_4OH, (300 nm, ϵ_M = 1990 $M^{-1} \cdot cm^{-1}$); *m*-ethylaniline in EC–PC, 0.7*M* NH_4OH, (291 nm, ϵ_M = 2060 $M^{-1} \cdot cm^{-1}$); 4-ethylpyridine in EC–PC, (255 nm, ϵ_M = 1675 $M^{-1} \cdot cm^{-1}$). A linear relationship between absorbance and polymer concentration was found for absorbances up to 1.5. PAN at 0.5 mg/mL was included in the solvent blank to correct for the small intrinsic absorbance of PAN structural defects in the 260–275 nm region.[25]

Membrane Casting and Characterization

To yield a viscosity suitable for membrane casting, polymers were dissolved in DMF using extensive mixing with a magnetic stirrer; in some cases, mechanical blending was required to decrease the viscosity of the polymer solution to a level suitable for casting. After filtration through Whatman #4 paper, thin films were spread onto dry chromic acid-washed glass plates with an 8-mil (203-μm) gate opening on a casting knife; this was followed by immediate aqueous coagulation at 2–5°C to minimize skin formation. Hydroxyl, aryl amine, and pyridyl polymer films were coagulated in deionized water, 0.1*M* HCl and 0.1*M* NH_4OH, respectively. Polymer solutions were stored at either ambient temperatures (hydroxyl polymers) or −20°C (aryl amine and pyridyl polymers). Membrane sheets were stored in 10 mM HCl, 0.02% NaN_3 at ambient temperatures. Care was taken to minimize the exposure of the aryl amine polymers and membrane sheets to light.

Membrane thickness was measured with a Peacock dial gauge, while membrane water content was estimated, after a quick dry-blotting of surface moisture, by weighing, drying in a vacuum oven, and reweighing of the dry membrane. Water flux was measured at 50 psig (345 kPa) of N_2 on 47 mm diameter membrane disks supported by a nonwoven, porous poly(ethylene terphthalate) cloth (Hollytex 3396 from Eaton-Dikeman).

Assuming that a membrane consists of an ensemble of identically sized cylindrical pores and that Poiseuille's law is applicable, an estimate of a membrane's average pore radius was calculated from

$$r = (8\eta lU/p\Phi Ak)^{0.5}$$

where r = pore radius (cm), η = solution viscosity (P), l = membrane thickness (cm), U = rate of fluid flow (mL/min), p = pressure (atm), Φ = void volume of membrane (%), A = membrane area (cm^2), and k = a units conversion factor of 6.08×10^7. The total number of pores in a membrane, N, is equal to the void volume of a membrane divided by the volume of a single pore,

$$N = Al\Phi/\pi r^2 l = A\Phi/\pi r^2$$

Thus, the total internal pore surface of a membrane, S, is

$$S = (2\pi rl) \times N = 2Al\Phi/r$$

Measurement of Membrane Pore Size Distributions

Individual solutions of seven dextran fractions of average molecular weight 4000, 10,500, 17,700, 40,000, 70,300, 252,000, and 2,000,000 were prepared at a concentration of 1.0 g/L in either 5.0 mM NaH_2PO_4 plus 0.005 w/v % NaN_3 or 0.02 w/v % NaN_3. After filtration through 0.2-μm cellulose triacetate membrane filters, the dextran solutions were pooled empirically to give a continuous, smooth distribution in molecular weight over the range 2000–2,000,000 (Fig. 1).

A pore size distribution analysis of a membrane was initiated by mounting a 43 mm diameter membrane on a porous nonwoven polyester support in

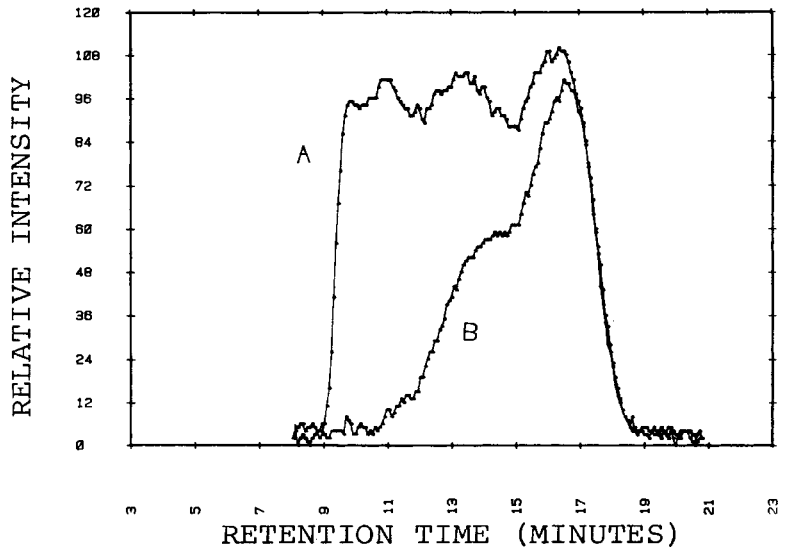

Fig. 1. Gel permeation chromatograph of the dextran feed (curve A) and permeate (curve B) from an acrylonitrile–4VP membrane. The dextran feed consisted of the seven dextran fractions pooled together in the proportions 15:5:22.5:20:5:15:35, from lowest to highest in molecular weight. For this series, the dextran samples were analyzed on the E-1000, E-1000, E-125 linked column configuration. The acrylonitrile–4VP membrane that was analyzed was cast from a 14 w/v % solution; the water and dextran fluxes were 56 and 15 $\mu m \cdot s^{-1} \cdot atm^{-1}$, respectively.

a stirred ultrafiltration cell (Amicon Corp.). About 75 mL of deionized water was pressure-driven at 10 psig through the membrane for 30–120 min, after which time a stable flux was measured. Next, the ultrafiltration cell was filled with 70 mL of the dextran pool solution and a pressure of 10 psig was reapplied. After the elapse of 20–45 min, the permeate stream was sampled, analyzed, and compared to the feed (Fig. 1).

Before disassembly of the ultrafiltration cell, a membrane was checked for possible pinholes and/or imperfections by pressurization with a solution of 1 mg/mL blue dextran of approximate molecular weight 2,000,000. The total retention of blue color, as judged by the absence of absorbance at 620 nm in the permeate, indicated structural integrity for membranes with water permeabilities of $<500\ \mu m \cdot s^{-1} \cdot atm^{-1}$. Higher flux membranes generally contained significant amounts of blue dextran in the permeate. This is to be expected since the membrane pores at the high end of the distribution are comparable in size to the molecular diameter of the smallest species of blue dextran.

The molecular weight distributions of the dextran permeate and feed were analyzed on a Waters liquid chromatogrphy system that consisted of a Waters 6000A pump, U6K injector, R401 refractive index detector, and three μBondagel size exclusion chromatography columns (either E-1000, E-125, E-high Å or E-1000, E-1000, E-125) connected in series as listed. Interfaced with the chromatography system was a Franklin Ace 100 microcomputer containing an Adalab analog/digital converter manufactured by IMI (Interactive Microware Inc., State College, Pa.), a disk drive, a monitor, and an Epson MX-100 dot matrix printer. A total of 1020 points per chromatogram was collected and stored on disk by sampling the detector at a rate of 80 times/min, beginning 8 min after sample injection.

The software for data manipulation and storage consisted of three program packages from IMI. "Vidisampler" provided for data manipulation with simultaneous background data acquisition, smoothed the experimental data via a 10-point smoothing cycle, corrected for detector baseline drift and imbalance, and calculated the percent rejection at each retention time. A user-augmented version of "Curve Fitter" then converted the retention times into pore radii as explained below and allowed for disk storage of the processed data. "Vidisampler" also allowed for disk storage of both the raw and processed data. Lastly, "Scientific Plotter" was used to plot and/or list the data in a user-specified format.

The percent rejection R_i is defined as

$$R_i = 100(F_i - P_i)/F_i$$

where F_i and P_i are the smoothed and baseline-adjusted signal intensities for the dextran feed and the permeate, respectively, at retention time i. A retention time was converted into a molecular size by means of a calibration curve constructed by the chromatography in tetrahydrofuran (THF) of polystyrene standards of known molecular weights and narrow molecular weight distributions. The experimental data were fit by a polynomial least squares analysis (Fig. 2). The molecular weight of the polystyrene was related to its molecular size by using the relation[26]

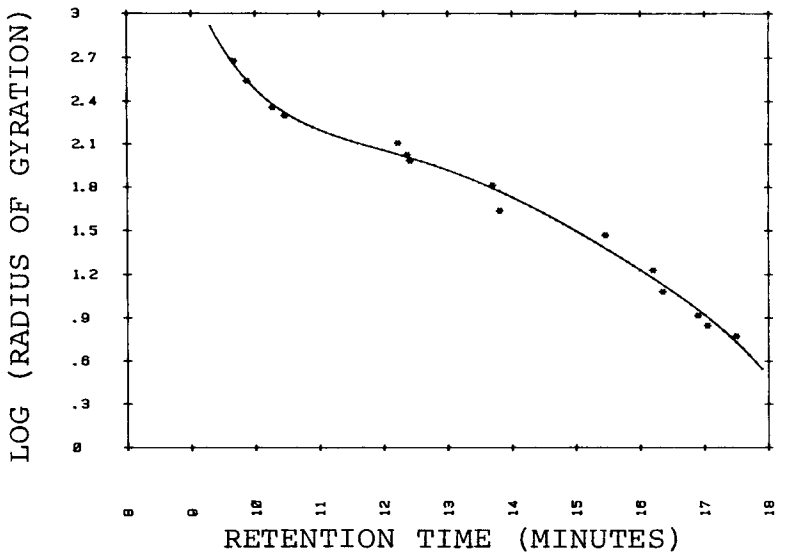

Fig. 2. Polystyrene calibration plot of E-1000, E-1000, and E-125 μBondagel columns linked in series. The curve is a fifth order polynomial fit for 15 polystyrene samples that cover the molecular weight range 600 to 1,030,000.

$$R_g = 0.137M^{0.589}$$

where R_g is the radius of gyration (Å) and M is the gel permeation chromatographic molecular weight. Although the calibration is strictly true only for a THF solvent system, the lack of a structural change in the silica beads' pore properties upon a change in solvent from THF to water implies that the calibration is also applicable for dextran in water. The ether-bonded silica column packing and dextran, as well as dextran and the various membrane copolymers, are assumed to be noninteractive; this allows for the conversion of a dextran molecular radius into a membrane pore radius. The validity of the latter assumption was supported by the return of ≥ 90 % of the initial water flux of a membrane after dextran analysis.

Ethylenediamine and Protein Coupling

EDA and CT were covalently attached to 47 mm diameter membrane disks after appropriate activation of the functional monomer in each copolymer. Pyridine containing membranes were activated with cyanogen bromide,[27] while aryl amine and hydroxyl containing membranes were activated with TsT in dioxane.[28] EDA was coupled to activated hydroxyl containing membranes in dioxane to prevent hydrolysis of triazinyl-chlorides.[28] The amount of EDA that coupled to a membrane was quantitated by ninhydrin analysis of dried membrane fragments, using EACA as a standard.

CT was coupled to activated membranes at pH 8.5 in aqueous buffer.[29] Solvent changes and membrane washings were accomplished at 50 psig by the mounting of a membrane in a stainless steel pressure filtration funnel (Gelman Science). Enzyme activity of immobilized CT was measured under continuous pumped-flow conditions at pH 8.5 with GPNA as a substrate.[30]

The protein loading of a membrane was determined by ninhydrin analysis[31] of an acid hydrolysate of a dried membrane, or quantitation of tryptophan in a base hydrolysate of a membrane.[32] Additional details of copolymer activation, protein/ligand coupling, and enzyme assay conditions are to be published.[33]

RESULTS

Copolymer Design and Synthesis

Seven distinct copolymers of acrylonitrile were synthesized to contain one of three different types of functional comonomers. The functional comonomer contained either an aryl amine (mAS, pAS), a pyridine (4VP, PEAM), or a hydroxyl group (HOPAM, HOPMAM, HDNMAM). Each type of comonomer permitted a different activation/coupling chemistry for protein-ligand immobilization.

A variety of factors were involved in chosing a comonomer, the comonomer concentration in the feed, and the polymerization conditions. Considerations included monomer reactivity ratios, availability of comonomers, stability of comonomers and copolymers, copolymer hydrophilicity, as well as the steric availability, the distance of a functional group from the backbone chain of the copolymer. Overriding these considerations in the design of a synthesis, however, was the copolymer's performance in making a membrane of suitable physical/structural stability with the desired porosity. This, in turn, depended very much on producing a polymer of sufficiently high molecular weight without conconmittant gel formation or post-polymerization crosslinking.

For hydroxyl-containing copolymers, the methacrylamide derivatives were found to be superior to the acrylamides. Besides having more favorable reactivity ratios, the methacrylamides gave fewer problems with crosslinking and polymer gelation after dissolution in DMF. Of the two methacrylamides, HDNMAM was expected to result in a more hydrophilic copolymer than HOPMAM; in addition, the increased length of the spacer arm in HDNMAM was a desirable feature for protein immobilization. However, there was a tendency for a crosslinked gel to form during the polymerizations with HDNMAM as compared with the formation of a crystalline glass-like polymer in the syntheses with HOPMAM. This limitation could be overcome by maintaining a low feed concentration of methacrylamide, such as $\leq$ 2 mol % HDNMAM and $\leq$ 5 mol % HOPMAM.

Molecular Weight of the Copolymers

Estimates of the molecular weight of several copolymers were obtained from intrinsic viscosity measurements. Such estimates were useful when polymerization conditions needed to be adjusted to result in the synthesis of a copolymer with viscosity in DMF appropriate for membrane casting. Since a definite measurement of the molecular weight was not required, concentration terms of order 2 and higher were ignored. The dependence of the intrinsic viscosity upon the molecular weight of the copolymer was assumed to be identical to that of a homopolymer of acrylonitrile.

The intrinsic viscosity of the copolymers in DMF ranged from 89.8 to 298 mL/g, depending on the particular polymerization conditions. Such intrinsic viscosities correspond to a weight-average molecular weight range of 60,000–300,000. Copolymers with an intrinsic viscosity of 120–200 mL/g were found to be the most suitable for the casting of unsupported membranes of the requisite physical stability and of the desired water permeability.

Copolymer Composition

The amount of pyridine or aniline comonomer incorporated into a copolymer was estimated by spectrophotometric analysis and by direct titration of acid polymer salts. Ultraviolet (UV) spectroscopy was used to obtain relative incorporation values for mAS, pAS, and 4VP comonomers. In all cases, the molar extinction coefficient of the comonomer after polymeric incorporation was taken as equal to that of an appropriately substituted nonpolymeric analog. For example, polyvinylpyridine and 4-ethylpyridine have been shown to have nearly identical extinction coefficients in dilute HCl.[34] In addition, the molar extinction coefficient of the aniline or pyridine comonomer in the copolymer was assumed to be invariant with its weight fraction in the polymer. Such has been found to be true for styrene–acrylonitrile copolymers when the mole fraction of styrene in the copolymer was ≥ 0.2[35]; extrapolation to zero styrene concentration, however, led to a negative extinction coefficient for the styrene. This may be attributed to the microstructure of the copolymer, among other factors. While such effects are also likely to be applicable for the aromatic chromophores of our copolymers, the assumption of a linear relationship between chromophore content and molar extinction coefficient over the limited mole fraction range under consideration, 0.01–0.15, is likely to be valid for the comparison of relative compositions, especially those involving different syntheses of the same copolymer.

UV absorbance spectra were recorded for pyridine and aniline copolymers in EC–PC or DMF (Fig. 3). The high absorbance of DMF in the far UV effectively limited spectra to wavelengths $\geq$ 270 nm. EC–PC, however, allowed the recording of spectra to about 240 nm.

All pyridine copolymers had an absorbance peak at 256–260 nm in EC–PC, irrespective of whether the pyridine existed as a free base or as an HCl salt. For copolymers of high 4VP content, however, the peak was considerably broadened in acidified EC–PC and shifted to the red; this may reflect the high charge density of the copolymer. The corresponding analog, 4-ethylpyridine, absorbed maximally in EC–PC and in acidified EC–PC at 255 and 254 nm, respectively.

The free base form of aniline copolymers had absorbance peaks in DMF at 296–297 nm and 293–296 nm for the *m*- and *p*-isomers, respectively. The addition of HCl protonated the aniline moities and led to the complete disappearance of the 290–300 nm peak. Spectra recorded in EC–PC were identical to those recorded in DMF except for a shift of the λ_{max} by several nm to lower wavelengths. The λ_{max} of the polymeric free base forms of mAS and pAS were red- and blue-shifted, respectively, by several nm from the λ_{max} of the appropriate ethyl analogs. The magnitude of the shift appeared to be proportional to the weight fraction of the aniline comonomer in the

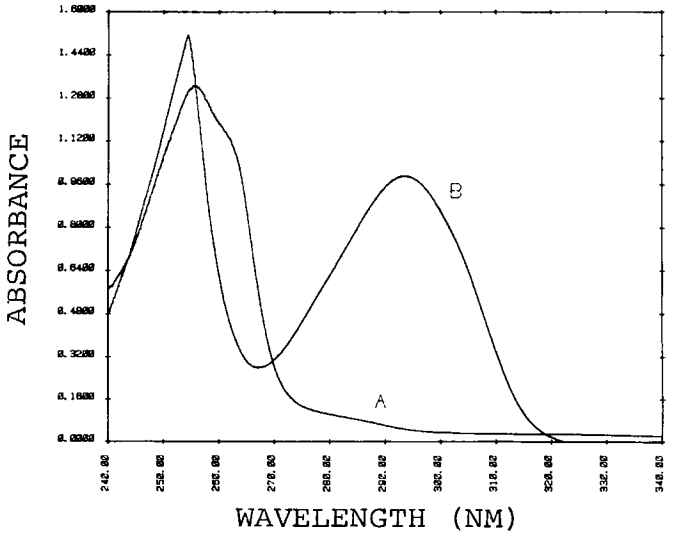

Fig. 3. Ultraviolet absorbance spectra of acrylonitrile–4VP (curve A) or acrylonitrile–mAS (curve B) copolymers in EC–PC.

polymer, especially for polymeric pAS. This is suggestive of an increasing self-interaction of the aromatic rings with the increasing polymeric ring density.

From the UV spectra, the mole ratio of mAS to acrylonitrile in the copolymers was estimated to be about 1.5 times that in the feed. For example, syntheses in which the mol % of mAS in the feed varied from 1.0 to 5.0 resulted in copolymers with a mAS content of 1.8–8.5 mol %. For pAS, however, the mole content of pAS in the polymer was always less than that in the feed by a factor of 2–3. A feed with 5.0 mol % pAS resulted in a copolymer with 1.9 mol % pAS. Since high molecular weight copolymers of pAS and acrylonitrile were difficult to obtain under the given synthetic conditions, most of the protein immobilization studies utilized mAS and not pAS copolymers.

Syntheses containing from 2.5 to 15 mol % 4VP in the feed resulted in copolymers containing from 3.0 to 20.5 mol % 4VP, respectively. The incorporation levels of 4VP are consistent with the reactivity ratios previously reported.[36]

Acid–base titrations of copolymers containing pyridine or aryl amine functional groups were performed in DMF. The base DTG, when dissolved in DMF, was suitable for the titration of perchlorate copolymer salts. Other solvents previously used in the titration of basic acrylonitrile copolymers[23,36] did not dissolve the high molecular weight copolymers described here.

The titration curves of several pyridine and aryl amine copolymers are presented in Figure 4. Negligible amounts of titratable acids were found in DMF only when it was freshly distilled before use. Homopolymers of acrylonitrile (PAN) contained a small amount (0.2 mol %) of titratable acids and this value was subtracted from all copolymer titrations.

In general, an acid–base titration led to a lower estimate of the polymeric content for a functional comonomer than a corresponding UV analysis. For

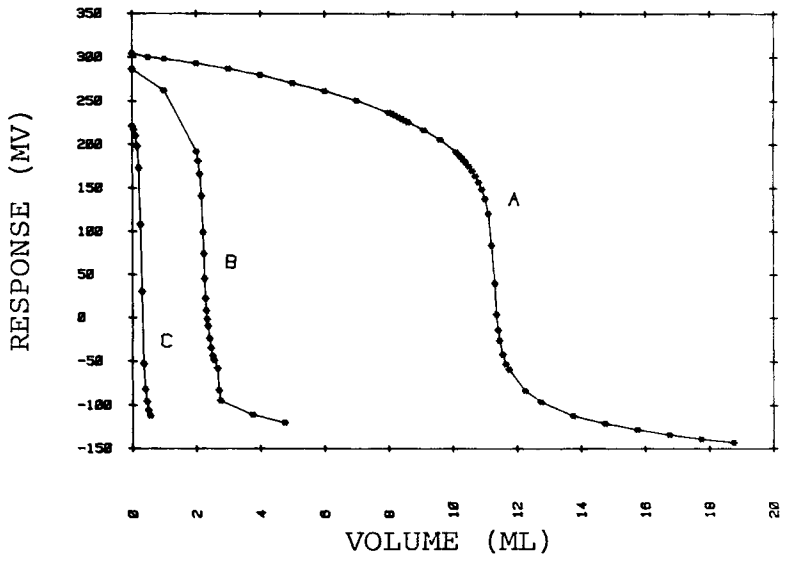

Fig. 4. Titration with DTG of the perchlorate salts of pAS– and 4VP–acrylonitrile copolymers. Curves A, B, and C were observed for 0.50 g of an acrylonitrile–4VP copolymer in 70 mL DMF, 0.74 g of an acrylonitrile–pAS copolymer in 70 mL DMF, and 0.41 g of PAN in 50 mL of DMF, respectively. Titration showed that the amounts of titratable acids were 6.0, 0.84, and 0.20 mol % for A, B, C, respectively.

example, an acrylonitrile–pAS copolymer with 5 mol % pAS in the feed gave 0.84 and 1.6 mol % pAS by titration and UV absorbance, respectively. In contrast, an acrylonitrile–4VP copolymer that contained 10 mol % 4VP in the feed gave 11.7 mol % by acid–base titration and 8.4 mol % by UV absorbance. Such discrepancies may arise from several sources. For example, titration with base may underestimate the true number of functional moieties in a polymer due to the loss of perchlorate during the rigorous washing and drying of the polymer acid salt. On the other hand, estimates based on the UV absorbance are likely to be in error largely due to the assumption of a linear relationship between chromophore concentration and molar extinction coefficient. Further investigations into these sources of error are in progress.

Relative Chemical Reactivity of Copolymers Containing Aryl Amines or Hydroxyl Groups

An hydroxyl-containing acrylonitrile copolymer contains neither a readily observable absorbance peak nor an acid-titratable group dependent on the hydroxyl comonomer contents. Estimates of the relative incorporation levels of the different hydroxyl comonomers, however, were obtainable by reaction of the copolymer with TsT (cyanuric chloride). To facilitate such reactions, the copolymer was first cast and coagulated into thin porous membranes.

TsT is quite reactive towards the hydroxyl groups of polysaccharides such as cellulose and agarose[37]; it also reacts very strongly with primary amines.[38] When such reactions are performed under conditions where TsT hydrolysis

is negligible,[39] a dichlorotriazine polymer derivative is formed. Subsequent reaction of the activated polymer with a large molar excess of a diamine such as EDA, again under nonhydrolytic conditions, results in the covalent coupling of 2 EDA molecules per activated site, neglecting any crosslinking mediated by the diamine and/or the TsT. The remaining free primary amine of EDA can then be readily quantitated with an amine sensitive reagent such as ninhydrin.

The results of such experiments with hydroxyl- and aryl amine-containing copolymers are summarized in Table I. Considering the two methacrylamide copolymers (HOPMAM and HDNMAM) as one group and mAS as another, there is a good correlation between the amount of EDA coupled and the amount of functional comonomer in the feed. This suggests that the reactivity ratios of acrylonitrile with HOPMAM and HDNMAM are comparable. In addition, the amount of polymer-incorporated mAS, as judged by UV absorbance, which in this instance is an independent assay of the number of functional groups, supports the direct relationship seen between TsT reactivity and functional comonomer composition.

The number obtained by this method for the amount of functional comonomer in a copolymer, however, is relative and not absolute. In the case of a mAS copolymer, only about 1/3 of the functional groups known to be present in the polymer, based on acid–base titration or UV absorbance, are reactive towards TsT. Presumably, this reflects an inaccessibility of some membrane polymeric aryl amines to TsT. An increase in either the TsT reaction time and/or temperature did not result in more coupling of EDA to mAS copolymers. For hydroxyl copolymers, on the other hand, such changes resulted in more EDA incorporation, but the more stringent re-

TABLE I
Reactivity of Hydroxyl and Aryl Amine Copolymers with TsT[a]

Functional comonomer	Mol % functional comonomer in feed	Nmol amine/ mg dry weight
HOPAM	3	158
HOPMAM	5	345
	5	390
HDNMAM	1	68
	1	29
	1.5	146
mAS	1 (2.0)	118
	3 (4.0)	214
	5 (8.5)	365

[a] Hydroxyl membranes were activated by incubation for 4 h at 50°C in dioxane made 0.1*M* TsT, 0.2*M* DIPEA; aryl amine membranes were activated for 30 min at ambient temperature with 0.05*M* TsT, 0.1*M* DIPEA in dioxane. After washing with dioxane, activated membranes were incubated with 1.0*M* EDA in dioxane for times exceeding 30 min. After further washing with dioxane and water, membranes were dried and the amine content quantitated with ninhydrin. PAN itself has a ninhydrin background of about 10–20 nmol/mg, presumably due to the formation of small quantities of primary amines during polymerization [50]. The same would likely be true for acrylonitrile copolymers; the above-tabulated values are not corrected for such a background. The mol % in parentheses are those observed for the copolymer based on absorbance at 295 nm.

action conditions resulted in membrane shrinkage and/or deformation. The EDA reaction was shown to proceed to completion in < 30 min at ambient temperatures, consistent with the results reported for TsT-modified agarose.[40]

Physical Characterization of Copolymeric Acrylonitrile Membranes

Thin films were cast from DMF solutions of different copolymer concentration. After coagulation, the membranes were characterized with respect to flux and physical properties. Typical data for the membranes obtained from an hydroxyl- and a pyridine-containing copolymer are presented in Tables II and III. These copolymers preparations produced membranes which encompassed the range of observable flux values. The large difference in the flux ranges can be largely attributed to the influence of polymer molecular weight on the membrane coagulation process.

As expected, the thickness of a membrane and the dry weight per unit area increased with the concentration of polymer in the casting solution. Water permeability, on the other hand, was inversely related to the concentration of the polymer in the casting solution. Estimates of the average pore radius derived from the water permeability indicated that the average pore diameter could be varied from 60 to 180 nm by adjustment of the coagulation conditions. Since most globular proteins have diameters between 5 and 20 nm, the average membrane pore was from 3 to 20 times larger than the immobilized protein, depending upon the particular membrane and protein under consideration.

Estimates of the internal membrane pore surface area were taken into account with respect to the desired polymeric content of functional groups. The number of functional groups on the pore surface needs to be high enough to maximize the loading of protein. However, the formation of an excessive number of sites for covalent attachment can lead to extensive crosslinking of an enzyme to a support matrix and consequent lowering of enzyme activity.[41] Modeling of protein loading as a cubicly close-packed

TABLE II
Properties of Acrylonitrile–HOPAM Membranes[a]

Membrane	Casting solution concentration (w/v %)			
	6.0	9.0	12.0	15.0
Thickness (μm)	92	102	110	112
Percent solids	11.3	12.9	15.1	20.1
Dry weight/membrane area (g/m^2)	8.0	11.5	16.8	23.2
Water permeability ($\mu m \cdot s^{-1} \cdot atm^{-1}$)	285	230	95	75
Pore size radius (nm)	49.0	46.5	32.0	29.0
Internal pore surface area/ membrane area	3360	3825	5870	6205
Internal pore surface area/ dry weight (m^2/g)	420	332	349	268

[a] The intrinsic viscosity of this copolymer was 298 mL/g. The mole ratio of the comonomers in the feed was 97:3 acrylonitrile:HOPAM.

TABLE III
Properties of Acrylonitrile–4VP Membranes[a]

Membrane	Casting solution concentration (w/v %)			
	7.0	9.1	11.9	14.0
Thickness (μm)	97	98	104	105
Percent solids	9.5	11.5	15.1	17.6
Dry weight/membrane area (g/m^2)	9.2	11.7	16.1	19.4
Water permeability ($\mu m \cdot s^{-1} \cdot atm^{-1}$)	925	700	530	295
Pore size radius (nm)	89.5	79.0	72.5	55.0
Internal pore surface area/ membrane area	1965	2190	2440	3145
Internal pore surface area/ dry weight (m^2/g)	215	187	152	162

[a] The intrinsic viscosity of this copolymer was 133 mL/g. The mole ratio of the comonomers in the feed was 10:90 acrylonitrile:4VP; UV absorbance showed the copolymer's composition to be 15.1 mol % 4VP.

monolayer on the internal pore surface of the membrane suggested that weight loadings of 15–30% were to be expected. In turn, assuming a random distribution of functional groups in the polymer, the density of functional groups on the surface was chosen such that after activation, from 5 to 20 sites of covalent attachment were theoretically possible between a protein molecule and the underlying membrane surface.

The microcomputer processing of the GPC elution profiles of the dextran pool and a corresponding membrane permeate led to a continuous smooth dextran rejection curve that covered the molecular weight range 2000–

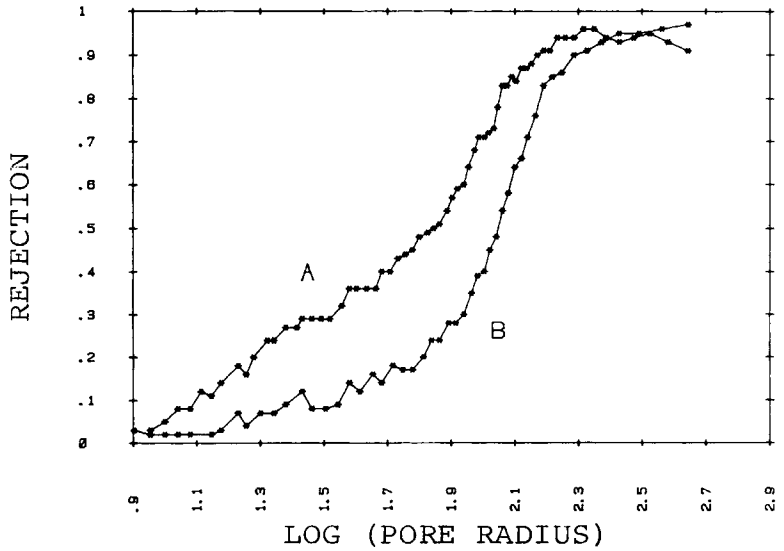

Fig. 5. Dextran rejection profiles for acrylonitrile–4VP membranes. Curves A and B were obtained for an acrylonitrile–4VP membranes cast from 14.0 and 11.9 w/v % copolymer solutions in DMF, respectively.

2,000,000. The rejection profiles of several copolymeric membranes as a function of molecular weight are shown in Figure 5. The sigmoidal shape of these profiles was typical for all membranes, although the extent of asymptotic character was dependent on the membrane coagulation conditions, especially coagulant bath temperature and polymer concentration. The rejection curves always had a pronounced asymptotic approach to 0% rejection and a linear region between about 40% and 85% rejection. At the high rejection end, curves either sharply leveled off at or approached asymtotically a rejection of ≥ 95 %. The % rejection of blue dextran of molcular weight 2,000,000 was used as an adjunct with respect to the value at which the dextran rejection curve leveled off. Such data indicate that a limiting asymptotic value of less than 100% rejection was an artifact, often attributable to a small mismatch in the retention times of the dextran feed and the membrane permeate before subtraction; a similar problem has been noted by Klein et al.[42] Thus, unless there was independent evidence to the contrary, a limiting rejection of ≥ 95 % was considered as equivalent to total rejection.

The linear midsection of a rejection curve was well described as a log-normal probability relationship.[43-45] The Stokes radius of the mean molecule for which $R = 0.5$ ranged from 4 to 15 nm, while the geometric standard deviation about the mean varied from 0.13 to 0.22 nm. While these standard deviations are larger than those reported for other polymeric membrane filters,[43] the three- to five-fold larger Stokes radius of the acrylonitrile-based membranes may account for the increase observed in the breadth of the distribution.

A log-normal distribution analysis clearly is insufficient in fully describing the complete pore size distribution, especially at the low and high rejection ends. In addition, the values for Stokes radius of the mean molecule are smaller than the average pore radii listed in Tables II and III by a factor of 3–5. While the latter are expected to be in error since they neglect factors such as membrane tortuosity and asymmetry, it remains to be determined whether the magnitude of the disagreement can be entirely explained by these factors.

The accessibility of pyridyl and aryl amine groups in a membrane was determined by back titration of the acid displaced from polymer salts. Such titrations showed that > 70 % of the functional groups known to be present in a membrane, as judged from the titration of an equivalent polymer salt dissolved in DMF, remained accessible to protons after coagulation into a membrane. Presumably, a smaller proportion of the total number of functional groups were accessible for molecules the size of a protein.

Protein Immobilization on Membranes

Chymotrypsin (CT) was immobilized upon the various types of copolymeric membranes described. This protein was selected because of the large body of available literature related to its structure–function relationships and its immobilization upon various types of matrix supports. CT is suited, particularly, as a model protein in immobilization studies because it can be assayed readily with low molecular weight synthetic substrates. An

amide substrate, GPNA, was employed using continuous, forced-flow circulation of substrate solution through a mounted 47 mm diameter membrane disk; the assay system was operated in a recycle reactor mode.

The functional groups of a membrane were activated with one of several appropriate reagents and subsequently loaded with protein by protocols described in detail elsewhere.[33] All membrane copolymers proved suitable for protein immobilization, although various copolymers differed with respect to the weight loading of enzyme upon a membrane. This "loading" value depended upon both the functional group concentration in a particular copolymer and the extent of activation. Maximal protein loading was observed routinely with acrylonitrile–mAS membranes, mainly as a result of their more rapid and extensive activation with TsT as compared with an equivalent hydroxyl-containing membrane. For example, the typical loading of CT on an acrylonitrile–mAS membrane was 1.5 g/m^2 of area, corresponding to a weight loading of 80 mg CT/g of total dry weight. The actual weight loading of protein on a membrane, however, was an intricate function of the conditions of membrane casting, with 15% weight loadings being observed on several occasions.

The total enzymatic activity of an average mAS membrane was 34.1 units/m^2 of area, where a unit is 1 μmol of product formed per minute at 25.0°C at pH 8.5. The specific activity of the immobilized CT was 0.024 units/mg of protein, which represents 42% of the activity of soluble enzyme towards GPNA. Preliminary studies suggest that the kinetics of membrane immobilized CT are not appreciably different from soluble CT.

The maximal loading capacity of hydroxyl and pyridine membranes for CT was about 80% and 25%, respectively, of that maximally observed with mAS-containing membranes. In all cases, the specific activity of the CT upon immobilization was between 40% and 65% of that of the initial soluble enzyme.

DISCUSSION

Reverse osmosis and ultrafiltration membranes made from polyacrylonitrile, or in some cases, acrylonitrile copolymers, have been well-studied and characterized. The acrylonitrile copolymers described herein were designed specifically for the immobilization of proteins upon membranes. The copolymer approach that was adopted allows for the incorporation of a comonomer containing a functional group for the covalent immobilization of a protein upon the membrane.

Many of the copolymers described have not been reported previously. This is especially true of the pAS- and mAS- containing copolymers. Direct synthesis of high molecular weight polymers containing these primary aryl amines is difficult[46] and is frequently circumvented by the nitration of polystyrene and the subsequent reduction of the polynitrostyrene.[47,48] In our experience, the rigorous exclusion of oxygen and the removal of polymerization inhibitors were crucial for syntheses with mAS and pAS.

Various copolymers have served as a matrix support in the immobilization of proteins.[2] However, the combination of a copolymeric matrix after configuration into a thin porous membrane and the direct covalent immobilization of a protein to that support appears unique.

An accurate appraisal of membrane pore size and size distribution was obtained from dextran rejection experiments. Such an analysis showed the majority of the membrane pores to be 3–20 times larger than the size of the majority of proteins envisioned for immobilization. Preliminary data show high loadings on our copolymeric membranes to be attainable for proteins as large as glucose isomerase (166,000 MW) and human IgG (150,000 MW).

Our dextran analysis is a significant extension of several previous protocols for measuring pore size distributions.[42,44,45,49] The analysis has been simplified and the range of measurable pore sizes increased by a factor of 10. This was achieved by pooling six different molecular weight fractions of dextran and by the analysis of the feed and permeate on linked GPC columns which resolved dextrans of molecular weight from 2000 to 2,000,000. Studies are in progress to correlate the dextran rejection profile with the rejection profile obtained for globular proteins.

References

1. R. A. Messing, *Immobilized Enzymes for Industrial Reactors,* Academic, New York, 1975.
2. I. Chibata, *Immobilized Enzymes: Research and Development,* Halsted, New York, 1978.
3. W. R. Vieth, K. Venkatasubramanian, A. Constantinides, and B. Davidson, in *Applied Biochemistry and Bioengineering* L. B. Wingard, Jr., E. Katchalski-Katzir, and L. Goldstein, Eds., Academic, New York, 1976, pp. 221–327.
4. K. Venkatasubramanian and W. R. Vieth, *Biotechnol. Bioeng.,* **15**, 583–588 (1973).
5. H. P. Gregor and P. W. Rauf, *Biotechnol. Bioeng.,* **17**, 445–449 (1975).
6. Y. Chen, N. S. Mason, R. E. Sparks, D. W. Scharp, and W. F. Ballinger, *Adv. Chem. Ser.,* **199**, 483–491 (1982).
7. A. C. Johanson and K. Mosbach, *Biochim. Biophys. Acta,* **370**, 339–347 (1974).
8. E. Staude and W. Jorisch, *Angew. Makromol. Chem.,* **96**, 21–36 (1981).
9. E. Staude, W. Jorisch, and W. Ansorge, *J. Membr. Sci.,* **11**, 289–296 (1982).
10. J. H. Reynolds, in *Immobilized Enzymes in Food and Microbiol Processes,* A. C. Ölson and C. L. Cooney, Eds., Plenum, New York, 1974, pp. 63–70.
11. B. S. Goldberg, A. G. Hausser, K. R. Gilman, and R. Y. Chen, *Am. Chem. Soc. Symp.,* **106**, 173–186 (1979).
12. O. R. Zaborsky, in *Immobilized Enzymes in Food and Microbiol Processes,* A. C. Olson and C. L. Cooney, Eds., Plenum, New York, 1974, pp. 187–203.
13. P. A. Biondi, M. Pace, O. Brenna, and P. G. Pietta, *Eur. J. Biochem.,* **61**, 171–174 (1976).
14. T. Handa, A. Hirose, S. Yoshida, and H. Tsuchiga, *Biotechnol. Bioeng.,* **24**, 1639–1652 (1982).
15. H. Miyama, T. Kobayashi, and Y. Nosaka, *Biotechnol. Bioeng.,* **24**, 2757–2763 (1982).
16. K. Matsumoto, R. Izumi, H. Seijo, and H. Mizuguchi, U. K. Pat. GB 2,015,001 (1979).
17. G. I. Tesser, H. U. Fisch, and R. Schwyzer, *Helv. Chim. Acta,* **57**, 1718–1730 (1974).
18. J. Lasch and R. Kolesch, *Eur. J. Biochem.,* **82**, 181–186 (1978).
19. J. Petit and R. Lumbroso, *C. R. Acad. Sci. (Paris),* **248**, 1541–1542 (1959).
20. P. Hardt, K. J. Boosen, and T. Voelker, Ger. Offen. 2,360,833 (1973).
21. W. K. Wilkinson, *Macromol. Synth.,* **2**, 78–81 (1978).
22. R. L. Cleland and W. H. Stockmayer, *J. Polym. Sci.,* **17**, 473–477 (1955).
23. C. A. Streuli, *Anal. Chem.,* **27**, 1827–1829 (1955).
24. I. M. Kolthoff, M. K. Chantooni, and H. Smagowski, *Anal. Chem.,* **42**, 1622–1628 (1970).
25. H. N. Friedlander, L. H. Peebles, Jr., J. Brandrup, and J. R. Kirby, *Macromolecules,* **1**, 79–86 (1968).
26. W. W. Yau, J. J. Kirkland, and D. D. Bly, *Modern Size Exclusion Liquid Chromatography—Practices of Gel Permeation and Gel Filtration Chromatography,* Wiley-Interscience, New York, 1979, p. 35.
27. F. Pittner, T. Miron, G. Pittner, and M. Wilchek, *J. Solid-Phase Biochem.,* **5**, 167–180 (1980).
28. L. T. Hodgins and M. Levy, *J. Chromatogr.,* **202**, 381–390 (1980).

29. J. R. Hildebrandt, A. Laccetti, A. Shamir, L. Hodgins, and H. P. Gregor, *Fed. Proc.*, **42**, 2068 (1983).
30. B. F. Erlanger, F. Edel, and A. G. Cooper, *Arch. Biochem. Biophys.*, **115**, 206–210 (1966).
31. S. Moore, *J. Biol. Chem.*, **243**, 6281–6283 (1968).
32. S. Blackburn, *Amino Acid Determination*, Marcel Dekker, New York, 1968, p. 193.
33. J. R. Hildebrandt, A. J. Laccetti, A. Shamir, L. T. Hodgins, and H. P. Gregor (1985), to appear.
34. H. B. Klevens, *J. Polym. Sci.*, **10**, 97–107 (1953).
35. L. H. Garcia-Rubio, *J. Appl. Polym. Sci.*, **27**, 2043–2052 (1982).
36. Y. Iwakura, T. Tamikado, M. Yamaguchi, and K. Takei, *J. Polym. Sci.*, **39**, 203–209 (1959).
37. G. Kay and E. M. Crook, *Nature*, **216**, 514–515 (1967).
38. J. T. Thurston, J. R. Dudley, D. W. Kaiser, I. Hechenbleikner, F. C. Schaefer, and D. Holm-Hansen, *J. Am. Chem. Soc.*, **73**, 2981–2983 (1951).
39. T. H. Finlay, V. Troll, M. Levy, A. J. Johnson, and L. T. Hodgins, *Anal. Biochem.*, **87**, 77–90 (1978).
40. T. H. Finlay, V. Troll, and L. T. Hodgins, *Anal. Biochem.*, **108**, 354–359 (1980).
41. A.-C. Koch-Schmidt and K. Mosbach, *Biochem.*, **16**, 2105–2109 (1977).
42. E. Klein, P. Feldhoff, T. Turnham, and R. P. Wendt, *J. Membr. Sci.*, **15**, 15–26 (1983).
43. A. S. Michaels, *Separation Sci. Technol.*, **15**, 1305–1322 (1980).
44. A. R. Cooper and D. S. Van Derveer, *Second World Filtration Congress*, (1979), pp. 455–461.
45. A. R. Cooper and D. S. Van Derveer, *Separation Sci. Technol.*, **14**, 551–556 (1979).
46. C. Kotlarchik and L. M. Minsk, *J. Polym. Sci., Polym. Chem. Ed.*, **13**, 1743–1744 (1975).
47. H. Filippusson and W. E. Hornby, *Biochem. J.*, **120**, 215–219 (1970).
48. G. Baum, *Biotechnol. Bioeng.*, **17**, 253–270 (1975).
49. H. H. Schwarz, E. Bossin, and D. Fanter, *J. Membr. Sci.*, **12**, 101–106 (1982).
50. J. Brandrup, J. R. Kirby, and L. H. Peebles, Jr., *Macromolecules*, **1**, 59–63 (1968).

Received December 21, 1983
Accepted March 28, 1984*

* Final author approval January 15, 1985.